A PHYSICS-BASED TEMPERATURE STABILIZATION CRITERION FOR THERMAL TESTING

Steven L. Rickman
NASA Engineering and Safety Center
NASA Johnson Space Center
Houston, TX

Eugene K. Ungar, Ph. D,
Crew and Thermal Systems Division
NASA Johnson Space Center
Houston, TX

ABSTRACT

Spacecraft testing specifications differ greatly in the criteria they specify for stability in thermal balance tests. Some specify a required temperature stabilization rate (the change in temperature per unit time, dT/dt), some specify that the final steady-state temperature be approached to within a specified difference, ΔT, and some specify a combination of the two. The particular values for temperature stabilization rate and final temperature difference also vary greatly between specification documents.

A one-size-fits-all temperature stabilization rate requirement does not yield consistent results for all test configurations because of differences in thermal mass and heat transfer to the environment. Applying a steady-state temperature difference requirement is problematic because the final test temperature is not accurately known a priori, especially for powered configurations.

In the present work, a simplified, lumped-mass analysis has been used to explore the applicability of these criteria. A new, user-friendly, physics-based approach is developed that allows the thermal engineer to determine when an acceptable level of temperature stabilization has been achieved. The stabilization criterion can be predicted pre-test but must be refined during test to allow verification that the defined level of temperature stabilization has been achieved.

INTRODUCTION

Thermal-vacuum testing of spacecraft and components always includes steady-state test objectives. One such test is a thermal balance test that is performed to correlate thermal math models. If a thermal balance test is not allowed to reach steady-state, the residual transient response prevents these data from being used in thermal math model correlation. Defining when

steady-VWDWH□ RFFXUV□ LV□ D□ EDODQFH□ EHWZHHQ□ JHWWLQJ□ ³FORVH□ HQRXJK´□ DQ needed to reach true steady-state. This balance becomes critical when the units under test are large and have long time constants. As the test articles approach spacecraft size the difference EHWZHHQ□ ³FORVH□ HQRXJK´□ DQG□ WUXH□ VWHDG\ state can add multiple days of very expensive, needless testing.

In the present work we explore the criteria that have been (and are) used to define steady-state in spacecraft thermal-vacuum testing. Numerous, often contradictory, criteria exist in test guidelines and requirements documents. Many of the documents give a minimum required rate of temperature change with time, dT/dt. However, a single value of dT/dt does not give the same result for all test articles because of differences in thermal mass and heat transfer to the environment. Many of the test documents define acceptable steady-state as reaching a temperature within a specified number of degrees of true steady-state. This is a logical choice since it specifies the accuracy of the measured temperatures as they are applied to steady-state models. However, the problem with this approach is that the true steady-state temperature is not known a priori, so the requirement cannot be applied directly during testing.

We present a new methodology to define acceptable steady-state in thermal-vacuum testing. The methodology uses a target temperature difference (ΔT_{target}) between acceptable steady-state and true steady-state, plus parameters that are measured during test to calculate an acceptable rate of temperature change. This method is a powerful, broadly applicable tool that can be used in thermal-vacuum testing to obtain acceptable steady-state measurements while minimizing test time.

BACKGROUND AND SURVEY OF TEMPERATURE STABILIZATION REQUIREMENTS

As part of this study, a variety of test requirements documents were surveyed [1,2,3,4,5]. The temperature stabilization criteria were expressed in a similar manner across all documents whereby temperature stabilization is achieved when a unit having the largest thermal time constant is within a specified ΔT of its steady-state value *and* the rate of change is less than a specified dT/dt. Some of the referenced documents suggest extrapolation of temperature trends to determine when a temperature within the prescribed ΔT has been reached while others recommend the use of previous temperature test data.

As is evident from the document survey, there are a variety of definitions for temperature stabilization. Temperature rate of change criteria* are specified but only reference time constants and thermal lag in terms of generalities. While general guidance is given, specifics on test data extrapolation are not provided. Also, extrapolation that is not based on physics is prone to problems. Steady-state temperatures are not known, except from analysis, so the difference from

* The specified temperature change rates, dT/dt, range from 1 °C/hr to 3 °C/hr in the documents surveyed.

the steady-state value is difficult to quantify accurately during the test. Incorrectly applying the temperature stabilization criteria, as written, could lead to early termination of a test that has not yet truly stabilized.

For a lumped-mass with only conduction or convection (i.e., linear) heat transfer, the time constant, τ_{linear}, is the product of the mass, m, and specific heat, c_p, divided by the sum of the linear conductances, ΣG, to the environment temperature:

$$\tau_{linear} = \frac{mc_p}{\Sigma G}$$

eq. 1

τ_{linear} is a measure of how rapidly a mass reacts to changes in the environment temperature and is expressed in units of time. A large time constant can arise from a high thermal inertia, mc_p, where a relatively large quantity of energy is required to raise the temperature of the mass. A large time constant can also arise when the sum of the conductances, ΣG, is small owing to restricted heat transfer to and from the mass. Additionally, the time constant is often variable in real-world problems due to variations in material properties and mechanical considerations affecting joint and interface conductances.

Contrary to the arbitrary specification of temperature difference and rate stabilization criteria presented in the cited requirements documents, the two are related. This complicating factor makes the published criteria difficult to apply. If the rate criterion is met, for example, the component may be nowhere near its steady-state temperature. Conversely, if the steady-state temperature criterion is met, the associated temperature change rate may be unacceptable per the specification. For example, a simple linear heat transfer model shows that a component with a time constant of 5 hours and a time rate change of temperature of 3 °C/hr (5.4 °F/hr) is 15 °C (27 °F) away from its steady-state temperature. To be within 3 °C (5.4 °F) of its true steady-state temperature (as required in Ref. 3, for example) the measured dT/dt would have to be less than 0.6 °C /hr (1.08 °F/hr); to be within 1 °C (1.8 °F) of the true steady-state temperature, dT/dt would have to be less than 0.2 °C/hr (0.36 °F/hr).

PROPOSED METHODOLOGY

The authors propose a methodology to address the difficulty of meeting the primary goal of a thermal balance test ± reaching steady-state within a small predetermined temperature band. The methodology applies to a powered or unpowered component that is exposed to one or more boundary temperatures through linear heat transfer or radiation or a combination of the two. The boundary temperatures can be radiation sink temperatures or temperature-controlled boundaries, such as base plates.

Consider a lumped-mass component in a thermal-vacuum test configuration with internal power generation, $\dot{Q}_{gen}$, and with radiation and linear heat transfer paths to a number of environment temperatures. The linear heat transfer, $\dot{Q}_C$, represented using a conductance, G, as

$$\dot{Q}_C = \sum_i G_i(T - T_{\infty_i})$$

eq. 2

where G_i represents the conductance of the heat transfer path to the i[th] sink, T is the component temperature, and T_{∞_i} represents the temperature of each heat sink.

Similarly, the radiation heat transfer, $\dot{Q}_R$, can be represented as the sum of the radiation interchange with a number of black body sink temperatures, T_{∞_j},

$$\dot{Q}_R = \sum_j \epsilon_j A_j \sigma F_j \left(T^4 - T_{\infty_j}^4\right)$$

eq. 3

where σ is the Stefan-Boltzman constant and ϵ_j, A_j, F_j, and $T_{\infty j}$are the emissivity, area, view factor, and sink temperature, respectively, that are associated with the j[th] radiation path[†].

An energy balance on the component yields

$$\dot{Q}_{gen} - \sum_i G_i(T - T_{\infty_i}) - \sum_j \epsilon_j A_j \sigma F_j \left(T^4 - T_{\infty_j}^4\right) = mc_p \frac{dT}{dt}$$

eq. 4

where m and c_p are the component mass and average specific heat, respectively.

We now introduce the steady-state temperature, T_{SS}, as an additional variable. A Taylor series expansion of T^4 about T_{SS} allows an exact solution to be obtained for eq. 4 which, in turn, allows derivation of the stability criterion. The Taylor series expansion is

$$T^4 = T_{SS}^4 + 4T_{SS}^3(T - T_{SS}) + 6T_{SS}^2(T - T_{SS})^2 + 4T_{SS}(T - T_{SS})^3 + (T - T_{SS})^4$$

eq. 5

[†] Alternatively, the interchange factor, B_j can be substituted for F_j to account for interchange with the sink via reflection off of other components. The final result of the derivation would be the same.

As the test article approaches steady-state, $(T - T_{SS})$ is necessarily small compared to T_{SS}, so the first two terms are an accurate approximation of T^4

$$T^4 \approx T_{SS}^4 + 4T_{SS}^3(T - T_{SS}) = 4T_{SS}^3 T - 3T_{SS}^4$$

eq. 6

Substituting the truncated expansion in eq. 4 yields

$$\dot{Q}_{gen} - \sum_i G_i(T - T_{\infty_i}) - \sum_j \epsilon_j A_j \sigma F_j \left(4T_{SS}^3 T - 3T_{SS}^4 - T_{\infty_j}^4\right) = mc_p \frac{dT}{dt}$$

eq. 7

or

$$\dot{Q}_{gen} - \sum_i G_i(T - T_{\infty_i}) + \sum_j \epsilon_j A_j \sigma F_j \left(3T_{SS}^4 + T_{\infty_j}^4\right) - \sum_j \epsilon_j A_j \sigma F_j 4T_{SS}^3 T = mc_p \frac{dT}{dt}$$

eq. 8

It can be seen from eq. 8 that the radiation term has been linearized. Grouping terms and rearranging results in a more convenient form

$$\frac{\dot{Q}_{gen} + \sum_i G_i T_{\infty_i} + \sum_j \epsilon_j A_j \sigma F_j \left(3T_{SS}^4 + T_{\infty_j}^4\right)}{\left[\sum_i G_i + \sum_j \epsilon_j A_j \sigma F_{,j} 4T_{SS}^3\right]} - T = \frac{mc_p}{\left[\sum_i G_i + \sum_j \epsilon_j A_j \sigma F_j 4T_{SS}^3\right]} \frac{dT}{dt}$$

eq. 9

where the coefficient on the right hand side of eq. 9 is the time constant. Here τ is

$$\tau = \frac{mc_p}{\left[\sum_i G_i + \sum_j \epsilon_j A_j \sigma F_j 4T_{SS}^3\right]}$$

eq. 10

Eq. 4 at steady-state is simply

$$\dot{Q}_{gen} = \sum_i G_i(T_{SS} - T_{\infty_i}) + \sum_j \epsilon_j A_j \sigma F_j \left(T_{SS}^4 - T_{\infty_j}^4\right)$$

eq. 11

When this expression for $\dot{Q}_{gen}$ is substituted into eq. 9, it reduces the first term to T_{SS}, the steady-state temperature. Eq. 9 is then recast as

$$T_{SS} - T = \tau \frac{dT}{dt}$$

eq. 12

This is a first order, linear differential equation with an exact solution

$$T = T_{SS} + (T_o - T_{SS})e^{-t/\tau}$$

eq. 13

where T_o is the temperature at t=0.

To develop the stability criterion, we take the derivative of eq. 13

$$\frac{dT}{dt} = -\frac{1}{\tau}(T_o - T_{SS})e^{-t/\tau}$$

eq. 14

and recombine it with eq. 13 itself to yield

$$\frac{dT}{dt} = -\frac{1}{\tau}(T - T_{SS})$$

eq. 15

At the target temperature, $T = T_{SS} - \Delta T_{\text{target}}$ in eq. 15 yields the target time rate change of temperature, $\left.\frac{dT}{dt}\right|_{target}$,

$$\left.\frac{dT}{dt}\right|_{target} = \frac{\Delta T_{\text{target}}}{\tau}$$

eq. 16

For a specified ΔT_{target}, we need the component time constant, τ to calculate $\left.\frac{dT}{dt}\right|_{target}$. The time constant can be computed from eq. 10 with pre-test knowledge of the component heating, geometry, materials, and construction plus details of its mounting and insulation. The component constituent masses and specific heats should be well known. However, the calculation of conductances is problematic since these normally consist of contact conductances and radiation through multi-layer insulation (MLI), neither of which is precisely known. This

leads to errors in the calculation of the conductances as well as errors in the pre-test prediction of T_{SS}. Because of these factors, the value of τ predicted pre-test should be relied on as only a pre-test guide. An accurate representation of the component time constant must be calculated real-time from data obtained during the normal course of a thermal-vacuum test. This calculation is detailed next.

Eq. 14 shows that the time rate change of temperature will take the form

$$\frac{dT}{dt} = Ae^{-t/\tau}$$

eq. 17

where A is a constant. If the time rate change of temperature is plotted vs. time during a test, τ can be calculated from an exponential curve fit. Thus the pre-test calculation of τ can be updated real-time. The updated value can then be used in eq. 16 to calculate the value of $\frac{dT}{dt}\Big|_{target}$ that will coincide with reaching the required ΔT_{target}.

If the test is a heat-up case, $dT/dt > 0$ and it can be plotted directly vs. time and curve fit to find τ. In the case of cool-down, $dT/dt < 0$, so its absolute value is plotted and curve fit to find τ. The resulting factor of -1 is incorporated in the lead coefficient of eq. 17.

Interestingly, the final steady-state temperature can be predicted at any time during the test by combining eqs. 13 and 14

$$T_{SS} = T + \tau\frac{dT}{dt}$$

eq. 18

so, the steady-state temperature can be predicted with knowledge of the time constant and the time rate change of temperature. Of course, the prediction becomes more accurate as steady-state is approached because:

- The truncated Taylor series expansion for T^4 (eq. 6) becomes more accurate
- The time constant is known with greater accuracy
- $\left|\frac{dT}{dt}\right|$ is smaller yielding a smaller temperature extrapolation

Thus eq. 18 can be used to accurately perform the extrapolation called for in the test specifications.

APPLICATION OF METHODOLOGY

Application of the proposed methodology is accomplished by executing the following steps:

1. Obtain the component time constant, τ, from *pre-test* analysis[Á] or by using eq. 10. This is a first approximation of the true time constant.

2. Specify a target temperature difference, ΔT_{target}, and calculate the preliminary temperature change value, $\left.\frac{dT}{dt}\right|_{target}$, associated with this temperature using eq. 16.

3. During the test, calculate the current component temperature time rate of change, $\frac{dT}{dt}$, from available test data. Perform an exponential curve fit of $\left|\frac{dT}{dt}\right|$ vs. t to refine τ.

4. Use the updated estimate of τ obtained in step 3 to refine $\left.\frac{dT}{dt}\right|_{target}$ as a termination criterion. Repeat as needed.

5. When $\frac{dT}{dt}$ measured during the test becomes less than the updated value of $\left.\frac{dT}{dt}\right|_{target}$, acceptable temperature stabilization has been achieved.

Application of this methodology results in knowledge that the temperature is within ΔT_{target} of the steady state temperature during test without knowing the true steady-state temperature beforehand.

TEST VALIDATION OF METHODOLOGY

A thermal-vacuum test was performed to validate the methodology. Two simple heated configurations were tested in separate runs in a thermal vacuum chamber: 1) heat transfer dominated by radiation to the chamber cold walls and 2) the dominant mode of heat transfer was conduction to a temperature-controlled plate.

Configuration 1 ± This test article was a heated cube constructed from 3.175 mm (0.125 in) thick aluminum plate. The cube measured 153 mm (6 in) on each side. Its surface was coated with two layers of Kapton® tape to improve its emissivity (ε = ~0.7). The cube contained six internal thermocouples ± one on each face. A small controlled conductive heat transfer path to the chamber wall was provided by a 0.305 m (1 ft) long Mylar®-covered 9.53 mm (3/8 in) outer diameter copper support tube with a 0.89 mm (0.035 in) wall thickness. Two thermocouples were mounted on the support tube to monitor heat flow. The cube included two internal 39 W

[‡] The temperature-time results of a pretest analysis provide $\left|\frac{dT}{dt}\right|$ vs. time. An exponential curve fit is used to calculate τ.

Kapton® film heaters mounted on opposite walls. These heaters were powered by a controlled direct current (DC) voltage source.

Configuration 2 ± This test article was similar to Configuration 1. It was made of aluminum and had the same size, thickness, and thermocouple and heater layout. A single layer of low ε aluminized Mylar® (ε = ~0.05) covered the box to reduce its radiation heat transfer. A single ¼ x 28 stainless steel bolt attached the cube to a 0.305 by 0.305 m (12 by 12 inch) 6.35 mm (1/4 inch) thick aluminum plate. The exposed plate was covered with Kapton® tape to improve its emissivity. Two Variac powered 125 W bar heaters were bolted to the underside of the plate. Three thermocouples were mounted on the plate to sense its temperature ± one in the center near the connecting bolt and two near the heaters.

The test configurations are depicted schematically in Figures 1 and 2. Photos of the actual test set-ups are presented in Figures 3 and 4. In the data discussion, the thermocouples are denoted DV³top´, ³bottom´, and ³VLGH´ corresponding to their relative locations in the chamber. The plate thermocouple near the bolt in Configuration 2 is taken as the plate temperature.

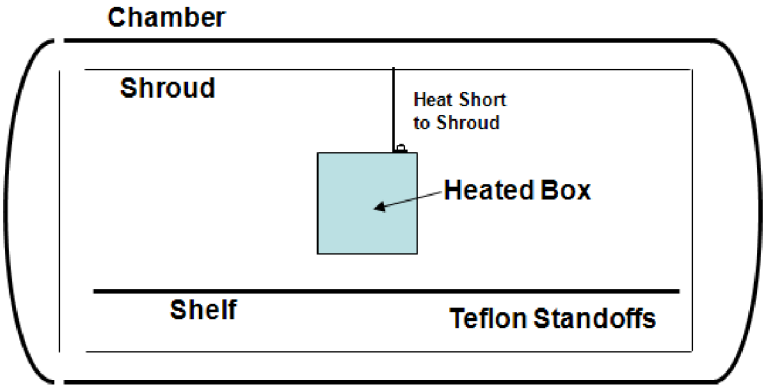

Figure 1 ± Test Configuration 1

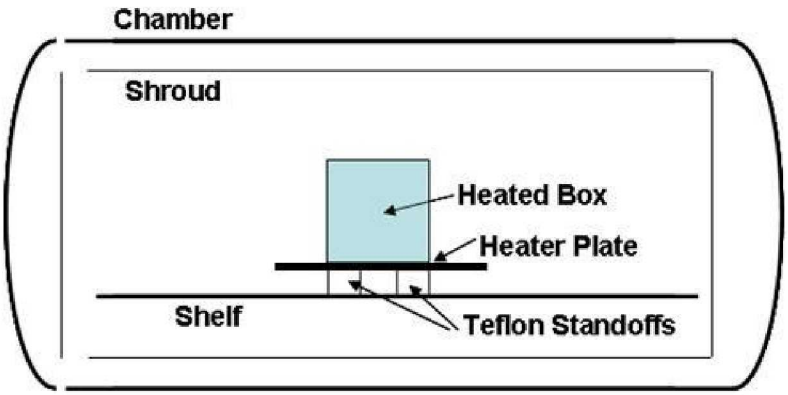

Figure 2 ± Test Configuration 2

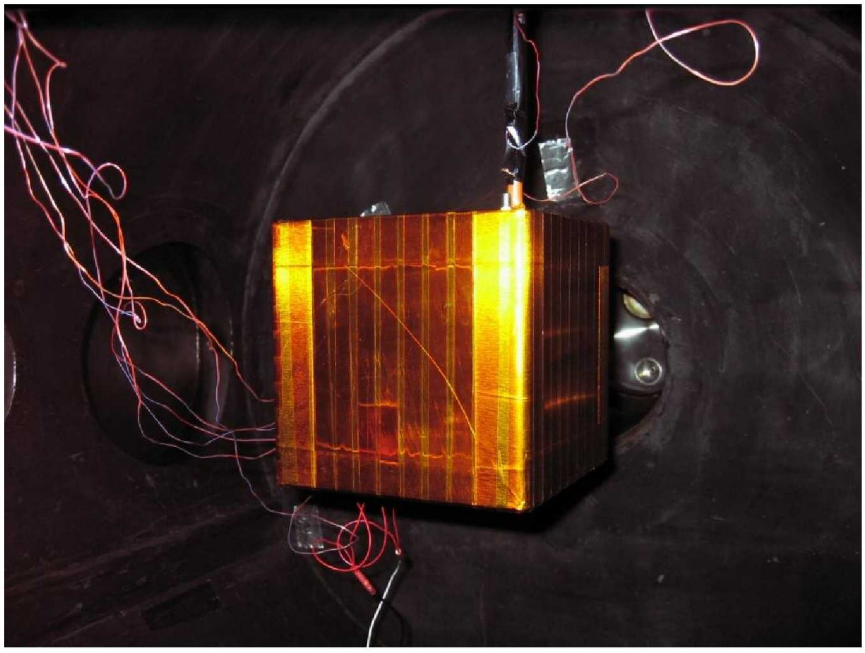

Figure 3 ± Test Configuration 1

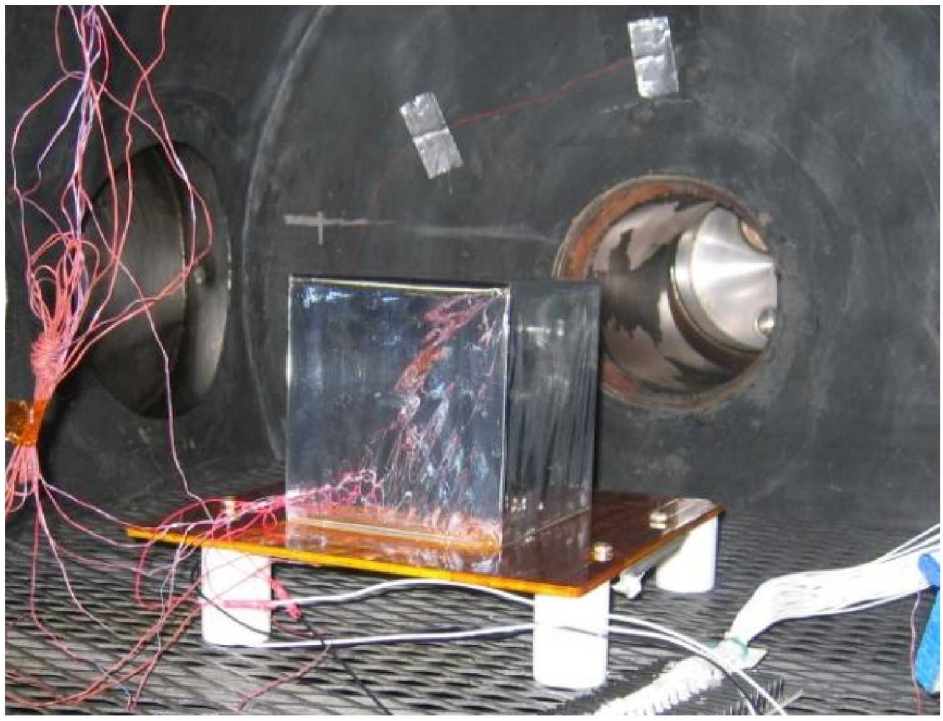

Figure 4 ± Test Configuration 2

After chamber pump-down to a pressure of less than 10^{-5} torr, the shroud was flooded with liquid nitrogen to control and maintain its temperature. Subsequently, the box heaters were powered on (as was the heater plate for Configuration 2). Temperatures were recorded and temperature change rates were calculated to allow application of the stabilization criteria methodology.

Once the steady state test objectives were completed, the chamber was returned to ambient conditions.

TEST RESULTS

A total of five test runs was made, all with an average measured shroud temperature of -165 °C (-266 °F).

Configuration 1 ± The Suspended Test Article (temperatures are approximate)

1. Heat-up from -49 °C to 30 °C (-56 to 85°F) under 60 W power
2. Cool-down from 27 °C to -14 °C (80 to 6°F) under 30 W power

Configuration 2 ± The Plate-Mounted Test Article (temperatures are approximate)

1. Heat-up from 27 °C to 63 °C (80 to 145 °F) under 32.4 W power
2. Cool-down from 50 °C to 47 °C (122 to 116 °F) under 14.9 W power

3. Heat-up from 43 °C to 46 °C (110 to 114 °F) under 14.9W power

A detailed discussion of the first test run of each configuration follows. All of the test runs behaved similarly - the time rate change of temperature, $\frac{dT}{dt}$ displayed the expected exponential form of $Ae^{-t/\tau}$ as the temperatures neared steady-state.

Configuration 1 - The suspended cube heat-up test temperature history is shown in Figure 5. The initial part of the plot is an unpowered cool-down. 60 W of heater power was applied at 0.533 hours. The six measured temperatures (one on each side of the box) show the expected asymptotic approach to the final temperature.

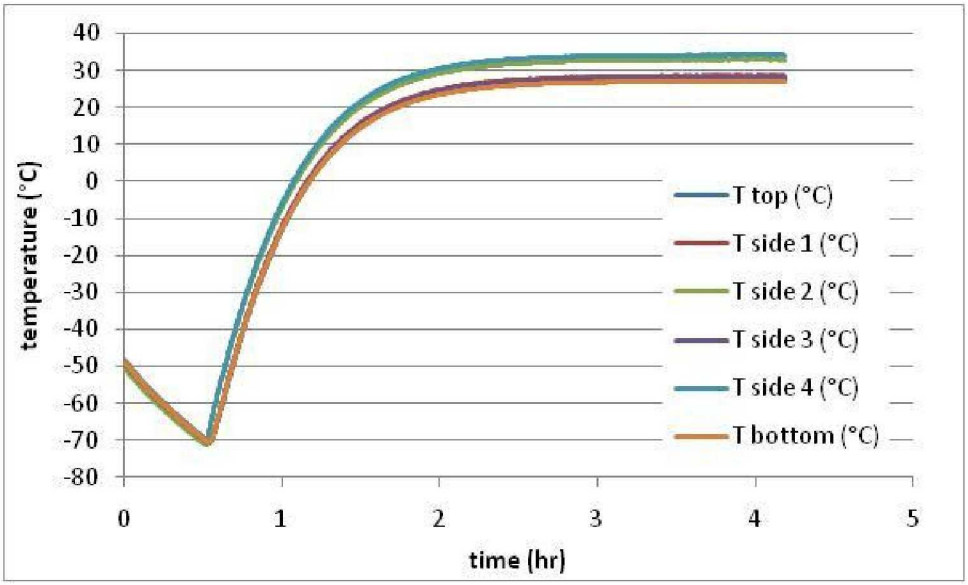

Figure 5 ± Hanging Cube Temperatures

Figure 6 shows the difference between the maximum recorded average temperature (taken as the steady-state average temperature) and the average measured temperature. The straight line nature of the plot after 1.5 hours shows that the exact exponential solution for temperature (eq. 13) will hold as steady-state is approached - as predicted by the theory. The increased scatter near the end of the test is caused by the increased relative effect of thermocouple measurement instabilities as steady-state is approached.

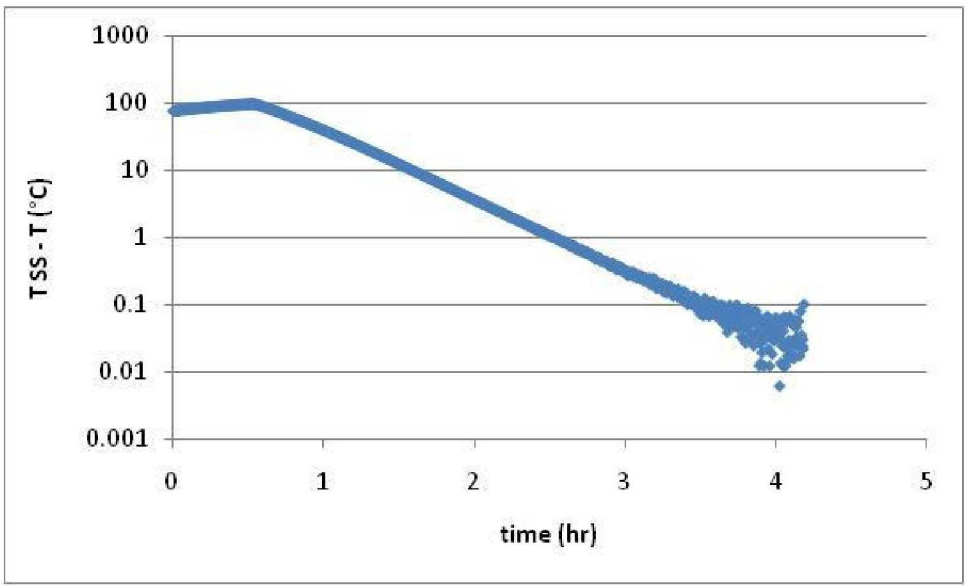

Figure 6 ± Hanging Cube Average Temperature Difference

The inverse of the slope of the straight line portion of the plot in Figure 6 is the time constant (an exponential curve fit yields $\tau = 0.426$ hours). However, this method of finding the time constant is not available during a test since the steady-state temperature is not known a priori. Instead, the method of plotting dT/dt real-time must be used. To mimic this methodology, the test data between 1.5 and 2.55 hours was analyzed as one would in real-time. First, the slope at each measurement point was calculated using a backwards difference of 5 minutes (i.e., the difference between a data point and the one taken five minutes previously was used to compute the slope at a particular time). The slopes were then plotted and curve fit with an exponential function to find the time constants. The plot for the cube top temperature is shown in Figure 7. The curve fit exponent is -2.488 hr^{-1}. Its inverse gives the time constant of 0.402 hrs.

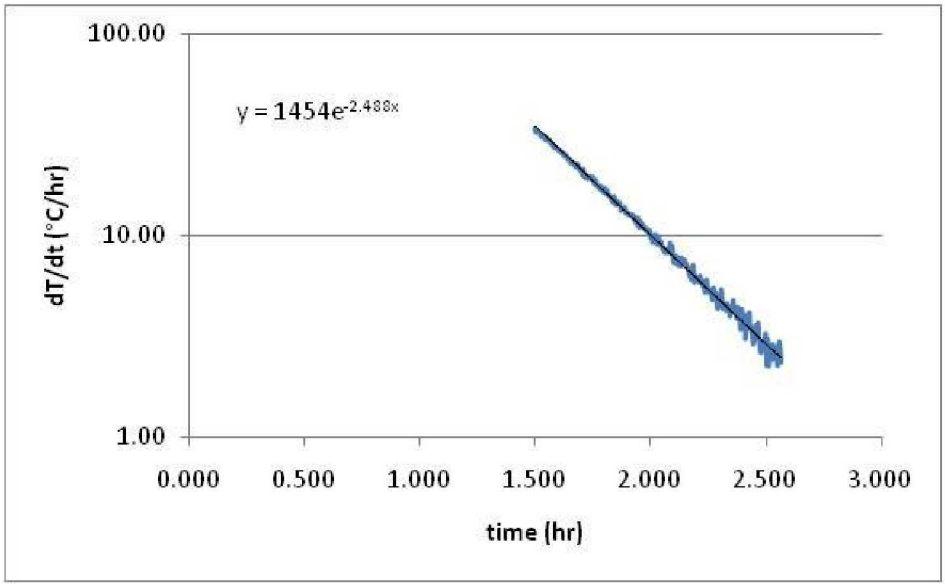

Figure 7 ± Time Rate Change of Temperature for the Top of the Hanging Cube Temperature

The time constants calculated in a similar fashion for all six thermocouple locations are listed in Table 1.

Table 1 ± Time Constants for The Hanging Cube
Calculated Real-Time

Location	Top	Side 1	Side 2	Side 3	Side 4	Bottom	Average Value
τ (hours)	0.402	0.373	0.410	0.401	0.405	0.402	0.399

The average time constant calculated for the cube is 0.399 hours ± within 7% of the time constant calculated from Figure 6. The real-time calculated value of $\tau = 0.399$ hours can be used to calculate the predicted steady-state temperature at any time during the test using eq. 18. These predicted temperatures are shown in Figure 8. The figure also shows the times where the temperature was expected to be within 1 °C and 0.5 °C of steady-state by the theory (2.65 and 2.85 hours, respectively). The agreement between theory and experiment is excellent.

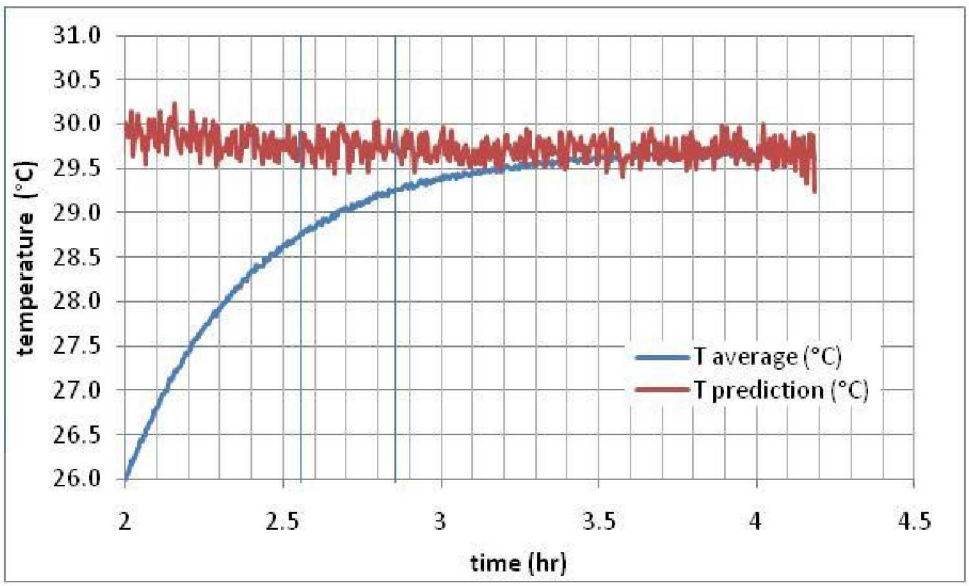

Figure 8- Measured Temperature and Predicted Temperature

The time constant for this test was also calculated from the hardware physical parameters using eq. 10. The computed value of 0.427 hours for this very simple configuration agrees well with the average value of 0.399 hours in Table 1 and the value of 0.426 hours from Figure 6.

Configuration 2 - The plate-mounted cube heat-up temperature history is shown in Figure 9. Prior to $t = 0$ the cube was unpowered and the plate was pre-conditioned to 22 °C (72 °F) by manually adjusting the Variac. At 0 hours, 32.4 W of heater power was applied to the cube and the Variac power was reduced. During the first part of the heat-up, the Variac power to the plate heaters was adjusted manually to maintain the measured plate temperature near 22°C (72 °F). The last Variac setting change (corresponding to a 5% increase in heater plate power to 35.4 W) occurred at 2.26 hours. After this point, no heater power levels were changed for the remainder of the test.

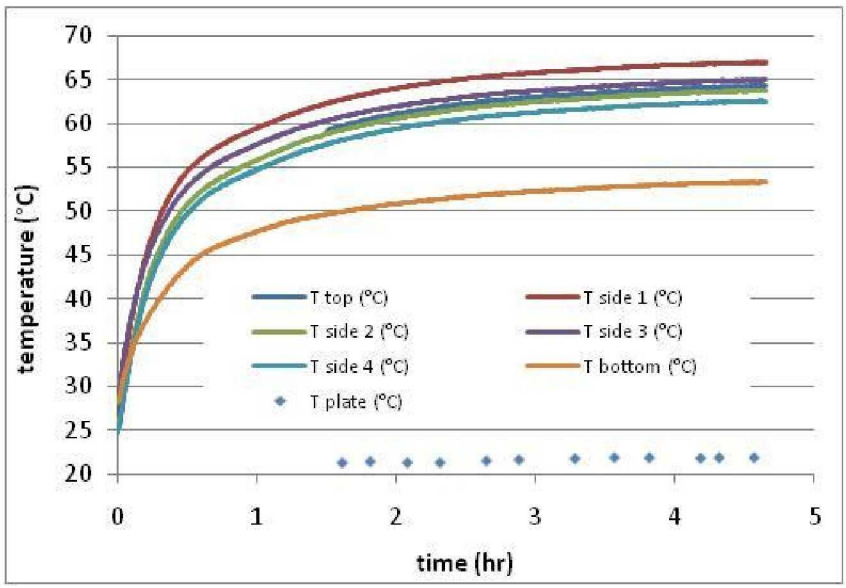

Figure 9 ± Plate-Mounted Cube Temperatures

The plate temperature measured near the cube mounting bolt (T_{plate}) shows a slight temperature increase during the latter portion of the test. The average increase after 2.26 hours is 0.223 °C/hour (0.402 °F/hour). This temperature rise is equivalent to 0.16 W of excess heating[§], which is negligible compared to both the 32.4 W of box heating and the 35.4 W of plate heating. However, this upward temperature creep must be removed from the data before stability can be assessed.

To remove the test temperature creep, we add a correction of $1.038 - 0.223\,t$ to all the temperature data after 2.26 hours. The correction is in °C and t is the elapsed time in hours. A sample of the data with and without the correction is shown in Figure 10.

[§] Based on the combined thermal mass of the test cube and the mounting plate.

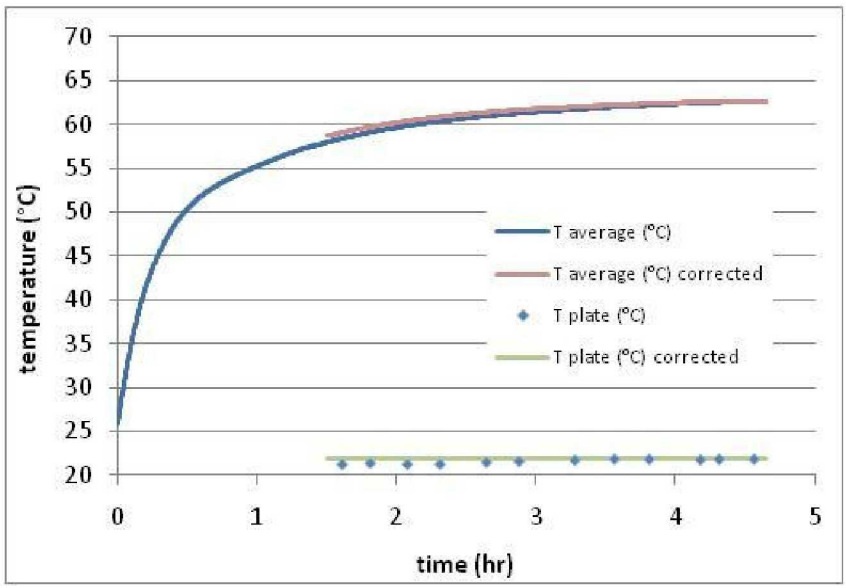

Figure 10 ± Raw and Corrected Average Cube Temperatures

The corrected temperature traces are shown in Figure 11.

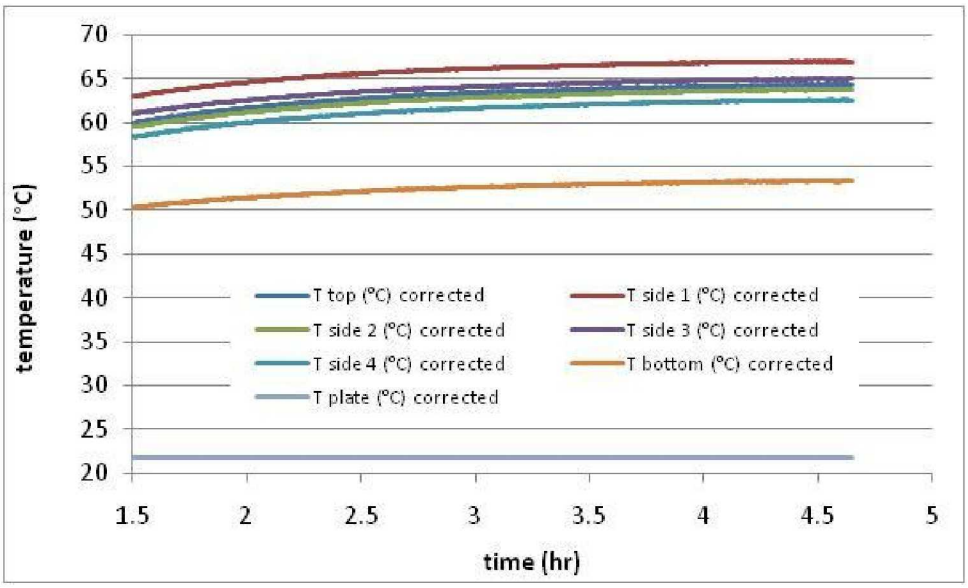

Figure 11 ± Corrected Plate-Mounted Cube Temperatures

To verify the methodology for this case, the corrected test data between 1.6 and 2.8 hours was analyzed as one would in real-time. First, the slope at each measurement point was determined using a backwards difference of 5 minutes. The slopes were then plotted and curve fit to find the time constants. The results for each thermocouple are listed in Table 2.

Table 2 ± Time Constants for the Plate-Mounted Cube
Calculated Real-Time

Location	Top	Side 1	Side 2	Side 3	Side 4	Bottom	Average Value
τ (hours)	1.036	1.076	1.015	1.053	1.040	1.076	1.049

The average time constant for the cube is 1.049 hours. As before, this time constant can be used at any time during the test to calculate the predicted steady-state temperature using eq. 18. The predicted temperatures are shown in Figure 12. The figure also shows the times where the current temperature was within 1 °C and 0.5 °C by the theory (3 and 3.8 hours, respectively). As before, the agreement between theory and experiment is excellent.

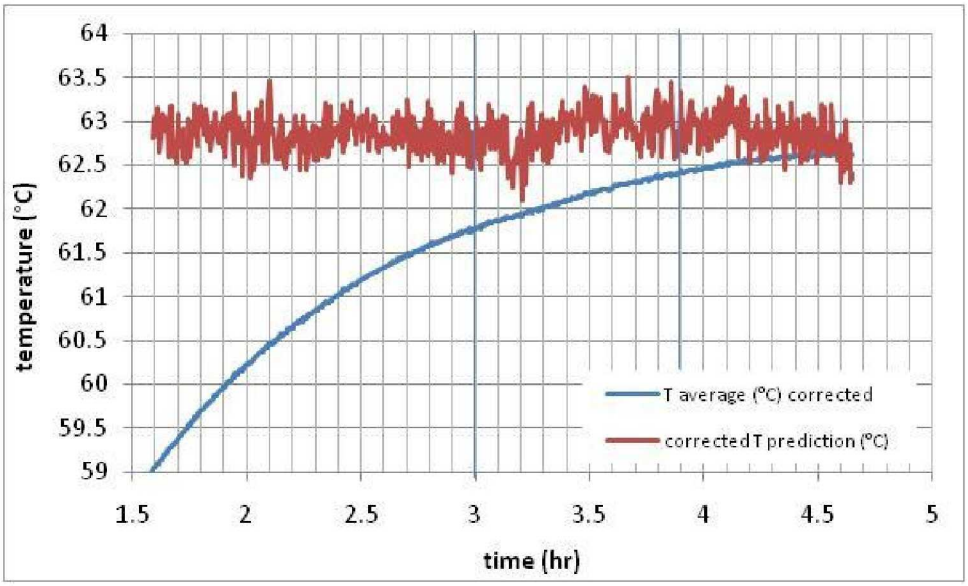

Figure 12- Measured Temperature and Predicted Temperature

The time constant for this test was also calculated from eq. 10 using the physical configuration. Based on a bolt interface resistance of 0.7 K/W[6] and a cube emissivity of 0.05, the value of the time constant for this test is 0.210 hours, which is in very poor agreement with the test calculated value of 1.049 hours. Even for this fairly simple configuration, the complication of a poorly known interface conductance makes the pre-test calculated value of τ inaccurate. However, by assessing τ during the test, an accurate value of the time constant can be obtained and the stability criterion can be applied accurately.

OTHER CONSIDERATIONS

For the methodology of the present work to be accurate, two conditions must be met: the unit under test must be thermally relaxed and the required time rate change of temperature must be measurable and readable. These conditions are discussed below.

Internal Thermal Relaxation ± A test article will have an internal thermal relaxation time constant, τ_{relax},

$$\tau_{relax} = \frac{L^2}{\alpha}$$

eq. 19

where L is a characteristic length of the unit and α LV□WKH□XQLW¶V□WKHUPDO□GLIIXVLYLW\□JL

$$\alpha = \frac{k_{eff}}{\rho_{eff} C_{p,eff}}$$

eq. 20

where k_{eff} , ρ_{eff}, and $c_{p,eff}$ are the effective thermal conductivity, density, and specific heat of the unit, respectively.

If the internal thermal relaxation time is much shorter than the time constant for heat transfer to the environment (eqs. 10 and 17), the unit will be thermally relaxed when the acceptable steady-state condition is reached.

Typical spacecraft components have internal thermal relaxation times on the order of one hour. Many hours are generally required for stability in thermal-vacuum testing, so the relaxation criterion is normally met. Table 3 lists the internal thermal relaxation times for representative active thermal control system components for the International Space Station (ISS), all of which are less than 1 hour.

Table 3 ± Typical ISS Active Thermal Control System Hardware Thermal Relaxation Time Constants

Component	Parent Material	Length (m)	Width (m)	Height (m)	L (m)	Parent Material α (m^2/s)	τ_{relax} (hr)
Heat Exchanger	Stainless Steel	0.55	0.51	0.17	0.08	3.79E-06	0.52
MBSU	Aluminum	0.92	0.82	0.50	0.25	8.90E-05	0.20
DDCU	Aluminum	0.88	0.77	0.56	0.28	8.90E-05	0.24
N_2 Tank	Aluminum	1.53	0.93	0.77	0.39	8.90E-05	0.47
NH_3 Tank	Aluminum	1.75	1.01	1.38	0.50	8.90E-05	0.79
NH_3 Pump Module	Aluminum	1.52	1.24	0.79	0.39	8.90E-05	0.48

Measurement Accuracy and Precision ± For massive components to meet reasonable stability requirements, the necessary time rate change of temperature may need to be less than 1 °C/hr. Normal data acquisition system level temperature measurement accuracy for resistance temperature detectors (RTDs) and thermocouples is no better than ±1.5 °C. Although the reading itself has a relatively large error, undisturbed RTDs and thermocouples can very accurately sense temperature *changes*. The standard accuracies quoted by the manufacturer[7] are ±0.005 °C/°C for RTDs and ±0.0075 to 0.015 °C/°C for thermocouples. This yields an instrument error of less than 1.5% when changes in temperature are measured. Data acquisition systems are also very stable. Because their error normally appears as an offset in the measured data, they too can yield accurate data for small temperature changes. If the data system is set up with sufficient granularity (i.e., bit flips at small enough intervals of temperature), it will yield data that provides an accurate measurement of the time rate change of temperature. This is especially true if graphical or averaging methods are used to smooth the digital data.

CONCLUDING REMARKS/RECOMMENDATION

A physics-based methodology for establishing thermal-vacuum test temperature stabilization has been developed and verified. The time constant of the test article is calculated pre-test, but must be updated during the test. With a refined time constant and a user-specified target temperature difference, a target time rate change of temperature is established. Once this rate is observed during test, the required temperature stabilization has been achieved. This methodology is a powerful, broadly applicable tool that can be used in thermal-vacuum testing to obtain acceptable steady-state measurements while minimizing test time. It is recommended that this technique be applied to properly couple the normally separate temperature stabilization criteria presented in the reviewed standards and requirements.

REFERENCES

1. Space Shuttle Specification, Environmental Acceptance Testing, SP-T-0023, Revision C, May 17, 2001.

2. Constellation Environmental Qualification and Acceptance Testing Requirements (CEQATR), CxP 70037 Revision B, Final, December, 17, 2008.

3. Qualification and Acceptance Environmental Test Requirements, International Space Station, SSP 41172, Revision Y, May 23, 2007.

4. Military Standard, Test Requirements for Launch, Upper Stage, and Space Vehicles, MIL-STD-1540C, September 15, 1994.

5. Department of Defense Test Method Standard for Experimental Engineering Consideration and Laboratory Tests, MIL-STD-810F, January 1, 2000.

6. Spacecraft Thermal Control Handbook, David G. Gilmore, Ed., 2nd Ed., The Aerospace Press, 2002.

7. The Omega® Temperature Measurement Handbook and Encyclopedia, Vol. MMX, 6th edition, Omega Engineering, Stamford, CT.

BIOGRAPHIES

Mr. Rickman is the NASA Technical Fellow for Passive Thermal and joined the NASA Engineering and Safety Center in 2009. In this capacity, he leads technical assessments for high risk programs and promotes stewardship of the passive thermal control and thermal protection disciplines. Previously, Mr. Rickman was the Chief of the Thermal Design Branch as the NASA ± Lyndon B. Johnson Space Center (JSC) where he led a group of more than forty civil servants and contractors focusing on passive thermal control and entry thermal protection, system and subsystem management for the Space Shuttle, International Space Station and Constellation programs, and entry thermal protection system testing. His interests include thermal analysis and passive thermal control of orbiting spacecraft. He has authored or co-authored a dozen publications including a chapter on natural and induced thermal environments for the textbook *Safety Design for Space Systems* (Elsevier, 2009). He holds a patent as a co-inventor of an innovative single-launch space station concept. Mr. Rickman earned a BS degree in Aerospace Engineering from the University of Cincinnati and a MS degree in Physical Science from the University of Houston at Clear Lake.

Dr. Ungar has degrees in mechanical engineering from the University of Cincinnati, the University of Kentucky, and the University of Houston. His dissertation was on boiling heat transfer. He has worked at NASA/JSC for the last twenty years in the area of single phase and

two-phase heat transfer and fluid flow. Over that time he has participated in the design, performance, and post-test analysis of numerous tests. He is a member of ASME.